



Momentum dependence and nodes of the superconducting gap in the iron pnictides

A. V. Chubukov,¹ M. G. Vavilov,¹ and A. B. Vorontsov²

¹Department of Physics, University of Wisconsin, Madison, Wisconsin 53706, USA

²Department of Physics, Montana State University, Bozeman, Montana 59717, USA

(Received 31 March 2009; revised manuscript received 1 October 2009; published 29 October 2009)

Using general symmetry arguments and model calculations we analyze the superconducting gap in materials with multiple Fermi-surface pockets, with applications to iron pnictides. We show that the gap in the pnictides has an extended s -wave symmetry but is either nodeless or has nodes, depending on the interplay between intraband and interband interactions. We argue that the nodes in the gap emerge without a phase transition as the tendency toward a spin-density-wave order gets weaker. These findings provide a way to reconcile seemingly conflicting results of numerical and experimental studies of the pnictides.

DOI: [10.1103/PhysRevB.80.140515](https://doi.org/10.1103/PhysRevB.80.140515)

PACS number(s): 74.20.Rp, 74.25.Nf, 74.62.Dh

I. INTRODUCTION

The structure of the superconducting order parameter is directly connected with interactions that produce the superconducting (SC) pairing. In conventional superconductors electron-phonon attraction leads to a fully gapped state. Electron-electron interactions are generally required to produce the gaps with the nodes, and the nodes were often interpreted as evidence for non- s -wave symmetry of the SC order parameter.

The symmetry and the structure of the SC gap are most controversial topics in the rapidly growing field of iron-based pnictide superconductors. Electronic band configuration of the pnictides assumes two hole pockets centered at the Γ point, $\mathbf{q}=(0,0)$, and two electron pockets centered at $(0,\pi)$ and $(\pi,0)$ in the unfolded Brillouin zone (BZ) to which we will refer in this Rapid Communication [Fig. 1(a)]. Multiple Fermi surfaces (FSs) create a number of different possibilities for the gap structures.^{1,2} Some numerical studies of itinerant³⁻⁶ and localized⁷ models predict nodeless gaps of different signs along the hole and electron FSs (an extended s^\pm state¹), while other studies predict an s^\pm state with nodes on electron FSs at smaller dopings and a $d_{x^2-y^2}$ state with nodes on hole FSs at larger dopings⁸ or a d_{xy} -type state⁹ with nodes on both hole and electron FSs. Experimental situation is also controversial: angular resolved photoemission spectroscopy (ARPES),¹⁰ thermal conductivity,¹¹ and penetration depth data^{12,13} on near-optimally electron or hole-doped FeAs materials can be explained assuming a nodeless s^\pm gap and interpocket impurity scattering,¹⁴⁻¹⁶ while penetration depth and thermal conductivity measurements on FeP-based LaOFeP (Refs. 17 and 18) and BaFe₂(As_{1-x}P_x)₂ (Ref. 19) unambiguously point on the presence of the nodes of the SC gap.

In this Rapid Communication, we show that both nodal and nodeless s^\pm gaps and a d -wave gap emerge within the same pairing scenario, depending on the interplay between intrapocket repulsion and interpocket pairing interactions the most relevant of which is the pair hopping between hole and electron FSs. Our key results are the following: if the pair hopping is stronger, the system develops an s^\pm gap without nodes. If the intrapocket repulsion is stronger, the system still develops an s^\pm gap but with nodes on the electron FSs, what allows the system to partly eliminate the effect of intrapocket

repulsion. The same interaction that leads to s^\pm state with nodes also yields an attraction in $d_{x^2-y^2}$ channel, which would give rise to a gap with the nodes along the hole FSs. We found, however, that, as long as pockets are small, s^\pm remains the primary instability although $d_{x^2-y^2}$ instability is a close second. At very large intrapocket repulsions, we found that the gap symmetry may change to d_{xy} because for such gap intrapocket repulsion completely disappears from the gap equation.

We argue below that the pair hopping is generally smaller than the intrapocket repulsion but is boosted by SDW fluctuations in systems where at zero doping the strongest instability is toward a nesting-driven SDW-type magnetism, and SC emerges when magnetism is destroyed by doping. In these systems, at low enough energies, pair hopping exceeds the intrapocket repulsion, and the s^\pm gap has no nodes. If the tendency toward SDW order is weaker at $x=0$, interpocket repulsion remains the largest down to the lowest energies, and the system develops an s^\pm gap with the nodes along electron FSs. We argue that the first case applies to near-optimally doped FeAs-based materials, while the second case applies to FeP-based and overdoped FeAs systems.

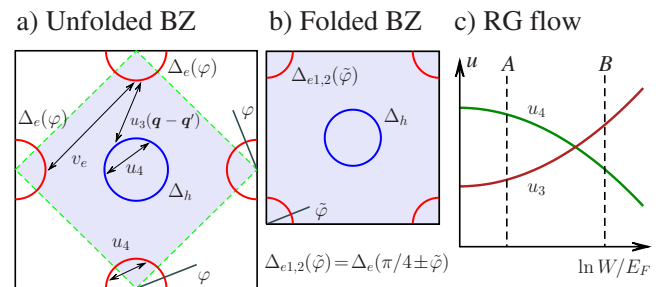


FIG. 1. (Color online) (a) Hole (center) and electron (edges) FSs in the unfolded BZ and interactions u_4 (intrapocket repulsion), u_3 (pair hopping between hole and electron bands) and v_e (pair hopping between electron bands). The s^\pm SC gap may have nodes along the dashed lines near the electron FS. (b) The folded BZ. Each corner now hosts two electron FSs with gaps $\Delta_{e1,2}(\tilde{\phi})$. (c) Schematic RG flow for u_4 and the momentum-independent part of $u_3(\mathbf{q}-\mathbf{q}')$ up to energies $\sim E_F$ (for $v_e=0$). If renormalized $u_3 > u_4$ (line B), the pairing occurs even if $u_3(\mathbf{q}-\mathbf{q}')=\text{const}$, while for $u_3 < u_4$ (line A) the pairing is induced by the momentum-dependent part of $u_3(\mathbf{q}-\mathbf{q}')$, and $\Delta_e(\varphi)$ has nodes.

II. PAIRING GLUE

Electron-phonon interaction is weak in Fe-pnictides²⁰ and the pairing is most likely due to the electron-electron interaction. The underlying electronic model for the pnictides involves Hubbard and exchange interactions between different Fe orbitals. In the “band description” which we will use, this model describes interacting fermions located near two hole FSs near (0,0) and two electron FSs near (0, π) and (π , 0) (the four-band model). The interactions relevant to the pairing are the Hubbard repulsion within hole and electron pockets, the hopping of electron pairs between hole and electron pockets, and the hopping of electron pairs between the two electron pockets and between the two hole pockets. For consistency with earlier works,⁵ we label these interactions as $u_4(\mathbf{q}-\mathbf{q}')$, $u_3(\mathbf{q}-\mathbf{q}')$, and $v_e(\mathbf{q}-\mathbf{q}')$ and $v_h(\mathbf{q}-\mathbf{q}')$, respectively, see Fig. 1(a). For simplicity we neglect the pair hopping v_h between the two hole pockets—for an s^\pm state its effect is the same as of u_4 . An angle-independent u_3 gives rise to a nodeless s^\pm state with the sign change of the gap between hole and electron FSs, however such state is only possible when u_3 is larger than u_4 and v_e terms which are both repulsive for s^\pm pairing (see below).

The bare value of u_4 derived from the underlying orbital model exceeds u_3 and v_e (Ref. 5). A simple reasoning for s^\pm gap then does not work. Earlier, several groups considered the case $v_e=0$ and argued^{4,5,21–23} that the difference u_4-u_3 may reverse sign and become negative (attractive) under the renormalization-group (RG) flow of the couplings from their bare values at the scale of the bandwidth W to the renormalized values at energies of order of Fermi energy E_F , which are actually relevant to the pairing. The reason for the sign change of u_4-u_3 is the boost given to u_3 from the coupling to density-density interaction which determines the tendency toward a spin-density-wave (SDW) order.^{5,22} When this tendency is strong, u_3 gets pushed up and overshoots u_4 between W and E_F , and the system develops an s^\pm gap without nodes. The same trend holds when $v_e \neq 0$.²³

New physics emerges when the tendency toward SDW is weaker, and the coupling in the s^\pm channel remains repulsive down to energies of order E_F . We show below that in this situation the system still develops an s^\pm pairing instability, this time due to momentum-dependent part of the pair-hopping term. This instability leads to an s^\pm gap with nodes on the two electron FS and occurs in the clean limit even at an arbitrary weak pair hopping. The reason why the pairing occurs despite strong repulsion is quite generic and is related to the fact that the gap that oscillates along the electron FS is insensitive to the intrapocket repulsion u_4 .⁸ The gap on the hole FS is still affected by u_4 , but it turns out that the elimination of the repulsion from the electron FS is a sufficient condition for the SC instability, still driven by the pair-hopping term between electron and hole FSs.

III. GAP EQUATION

We label fermions near different FSs as $f_{1,2}$ (hole) and $c_{1,2}$ (electron) and label the gaps as $\Delta_h(\mathbf{q})$ and $\Delta_e(\mathbf{q})$. The gaps along the two electron FSs transform into each other under rotations by $\pi/2(x \rightarrow y)$ and reflections. For simplicity, we

consider the case when the gaps $\Delta_h(\mathbf{q})$ on the two hole FSs are equal, the extension to the case of nonequal gaps is straightforward. The pairing interactions are $\sum_{i=1,2} u_4(\mathbf{q}-\mathbf{q}') (c_{i,q}^\dagger c_{i,-q}^\dagger c_{i,q'} c_{i,-q'} + f_{i,q}^\dagger f_{i,-q}^\dagger f_{i,q'} f_{i,-q'})$ (intra-pocket), $\sum_{i,j=1,2} u_3(\mathbf{q}-\mathbf{q}') c_{i,q}^\dagger c_{i,-q}^\dagger f_{j,q'} f_{j,-q'} + \text{H.c.}$ (between hole and electron pockets), and $\sum_{i \neq j} v_e(\mathbf{q}-\mathbf{q}') f_{i,q}^\dagger f_{i,-q}^\dagger f_{j,q'} f_{j,-q'} + \text{H.c.}$ (between the two electron pockets), where in all cases \mathbf{q} and \mathbf{q}' are on the FSs (we omit spin indices and consider a singlet pairing). The angle dependences of the interactions are strong because of strong variation in the weighting of different orbital harmonics along the FSs (Ref. 24) and in general no regular expansion is possible. However, when hole and electron pockets are small, as in pnictides, the angle variation can be cast in the expansion in powers of $k_F^2 \ll 1$ (we set interatomic distance to one). Functions $u_3(\mathbf{q}-\mathbf{q}')$, $u_4(\mathbf{q}-\mathbf{q}')$, and $v_e(\mathbf{q}-\mathbf{q}')$ have projections onto one-dimensional (1D) A_{1g} (s -wave), B_{1g} , and B_{2g} (d -wave), and two-dimensional (2D) E (p -wave) representations. We focus on 1D representations, where attraction is possible. Without loss of generality, we can set $u_4(\mathbf{q}-\mathbf{q}')$ and $v_e(\mathbf{q}-\mathbf{q}')$ to be constants u_4 and v_e and include the angle dependence from u_3 . We have

$$\begin{aligned} u_3(\mathbf{q}-\mathbf{q}') &= u_3 + 2\bar{u}_3[\cos(q_x - q'_x) + \cos(q_y - q'_y)] \\ &= u_3 + \bar{u}_3[(\cos q_x + \cos q_y)(\cos q'_x + \cos q'_y) \\ &\quad + (\cos q_x - \cos q_y)(\cos q'_x - \cos q'_y)] + \dots, \end{aligned} \quad (1)$$

where dots stand for 2D representations and 1D terms whose contributions to the pairing are smaller in k_F^2 . To the same approximation, $u_3^{A_{1g}} \approx u_3 + \sqrt{2}\bar{u}_3 \cos 2\varphi$ and $u_3^{B_{1g}} = \sqrt{2}\bar{u}_3 \cos 2\varphi$, where $\bar{u}_3 = \bar{u}_3 k_F^2 / (2\sqrt{2})$.²⁵

We assume that the couplings are already renormalized by fermions with energies between W and E_F and consider the system behavior below E_F when the pairing and SDW channels are decoupled, and the SC can be treated within the BCS approximation. The set of the coupled BCS equations for $\Delta_h(\mathbf{q})$ and $\Delta_e(\mathbf{q})$ is obtained in the standard manner. Consider first A_{1g} channel. On the hole FSs $\Delta_h(\mathbf{q}) \approx \Delta_h$ is approximately constant while on electron FSs $\Delta_e(\mathbf{q}) = \Delta_e + \bar{\Delta}_e(\cos q_x + \cos q_y) \approx \Delta_e + \bar{\Delta}_e \sqrt{2} \cos 2\varphi$ with $\bar{\Delta}_e = k_F^2 \bar{\Delta}_e / 2\sqrt{2}$. The coupled linearized equations for three gaps Δ_h , Δ_e , and $\bar{\Delta}_e$ are (we take all FSs as cylindrical)

$$\Delta_h = -u_4 L \Delta_h - u_3 L \Delta_e - \bar{u}_3 L \bar{\Delta}_e, \quad (2a)$$

$$\Delta_e = -u_4 L \Delta_e - u_3 L \Delta_h - v_e L \Delta_e, \quad (2b)$$

$$\bar{\Delta}_e = -\bar{u}_3 L \Delta_h + v_e L \bar{\Delta}_e, \quad (2c)$$

where $L = \ln(\Lambda/T_c)$ and $\Lambda \sim E_F$ is the upper energy cutoff. From Eqs. (2) we obtain the equation for the critical temperature T_c in the form

$$\begin{aligned} &\{(1 + u_4 L)[1 + (u_4 + v_e)L] - u_3^2 L^2\}(1 - v_e L) \\ &= \bar{u}_3^2 L^2 [1 + (u_4 + v_e)L]. \end{aligned} \quad (3)$$

It is invariant with respect to sign change of \bar{u}_3 and u_3 .

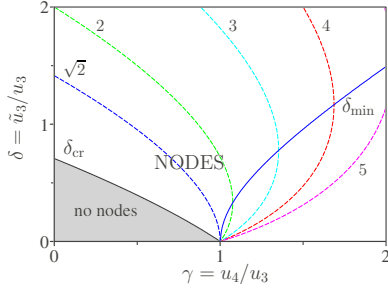


FIG. 2. (Color online). The phase diagram in dimensionless variables $\gamma = u_4/u_3$ and $\delta = \tilde{u}_3/u_3$ (we set $v_e = 0$). The nodeless s^\pm state exists in the lower left corner below the line $\delta_{cr}(\gamma)$, when intraband repulsion u_4 and momentum-dependent interband hopping \tilde{u}_3 are small. Dashed lines show the contours of fixed ratio $\tilde{\Delta}_e/\Delta_e = \sqrt{2}, 2, 3, 4, 5$. The narrow solid line shows the position of a minimum of $\tilde{\Delta}_e/\Delta_e$ in the region where the gap has nodes. Below this line, the gap develops nodes primarily to reduce the effect of intrapocket repulsion.

The gap that emerges at T_c has generally nonzero Δ_h , Δ_e , and $\tilde{\Delta}_e$. Their ratios are

$$\frac{\tilde{\Delta}_e}{\Delta_e} = \frac{\tilde{u}_3}{u_3} \frac{1 + (u_4 + v_e)L}{1 - v_e L}, \quad \frac{\Delta_e}{\Delta_h} = - \frac{u_3 L}{1 + (u_4 + v_e)L}, \quad (4)$$

where L is a solution of Eq. (3). Note that Δ_e and Δ_h have opposite signs if $u_3 > 0$. When the ratio $\tilde{\Delta}_e/\Delta_e < 1/\sqrt{2}$, the s^\pm state has no nodes, otherwise there are nodes on the electron FS.

For $\tilde{u}_3 = 0$, Eq. (3) has two solutions: one at $L = L_0 = 1/(\sqrt{u_3^2 + v_e^2/4} - u_4 - v_e/2)$ yields a nodeless s^\pm gap with $\Delta_e = -\Delta_h$ and $\tilde{\Delta}_e = 0$, another $L = L_1 = 1/v_e$ is entirely due to v_e and yields the gap which vanishes along the hole FS and oscillates as $\cos 2\phi$ along the electron FSs. The second solution is inconsistent with ARPES which clearly shows that the gap along hole FSs is nonzero and we therefore focus on the first solution and its evolution with \tilde{u}_3 . Such solution exists only if $u_3^2 > u_4(u_4 + v_e)$ and is impossible without RG flow as at the bare level u_4 is the largest coupling.

We now consider what is the fate of the solution $\Delta_e = -\Delta_h$, $\tilde{\Delta}_e = 0$ when the momentum-dependent part of the interaction $\tilde{u}_3 \neq 0$. Equation (3) at $\tilde{u}_3 \neq 0$ is a cubic equation in L , and we analyzed it for arbitrary values of parameters. We found that v_e sets the lower cutoff at $L = 1/v_e$ for the solution with the nodes (see below), while the physics can be fully captured without v_e . To simplify the presentation, we then set $v_e = 0$, introduce $\delta = \tilde{u}_3/u_3$ and $\gamma = u_4/u_3$ and obtain the full phase diagram in variables δ and γ (see Fig. 2).

For $\gamma < 1$, T_c is finite already at $\delta = 0$ and gradually increases with δ together with the oscillating component $\tilde{\Delta}_e$. The nodes on the electron FS appear above some critical $\delta_{cr}(\gamma)$, see Fig. 2 [$\delta_{cr}(\gamma \ll 1) \approx 1/\sqrt{2} - \gamma/\sqrt{3}$ and $\delta_{cr}(\gamma \approx 1) \approx \sqrt{8/9(1-\gamma)}$].

For $\gamma \geq 1$, we found different behavior: superconductivity develops discontinuously for $\delta \neq 0$. Indeed, the right-hand side (rhs) of Eq. (3) scales as $u_3^2(\gamma^2 - 1)L^2$ at $L \gg 1$, while the

left-hand side (lhs) scales as $u_3^3 \gamma \delta^2 L^3$, i.e., it has higher power of L . Comparing the two, we find $L = (\gamma^2 - 1)/(u_3 \delta^2 \gamma)$, i.e., $T_c = \Lambda \exp[-(\gamma^2 - 1)/(u_3 \gamma \delta^2)]$. The oscillating component of the gap $\tilde{\Delta}_e$ now dominates and exceeds both Δ_h and Δ_e by $1/\delta$. The physical reason why T_c is nonzero despite strong intrapocket repulsion is the absence of the $u_4 \tilde{\Delta}_e$ term in Eq. (2c) because the angular integral of $\tilde{\Delta}_e(\phi)$ vanishes. In other words, oscillations of the gap along the electron FS allow the system to develop SC order in spite of a strong intrapocket repulsion.

The important feature of the phase diagram is the qualitative change in the system behavior near $\gamma \approx 1$ and at $\delta \ll 1$. In this region $\tilde{\Delta}_e/\Delta_e = [\sqrt{2\delta^2 + (1-\gamma)^2} + (\gamma-1)]/\delta$ is nearly discontinuous, evolving from $\mathcal{O}(\delta)$ at $\gamma < 1$ to $\sqrt{2}$ at $\gamma = 1$, and to $\mathcal{O}(1/\delta)$ at $\gamma > 1$, i.e., the gap rapidly changes its form and develops the nodes.

On a more careful look, we find two sub-regimes for $\gamma > 1$, when the gap has nodes. One is the regime of small δ , where the gap is fully adjusted to minimize the effect of repulsive u_4 . In this regime, $\tilde{\Delta}_e \gg \Delta_e, \Delta_h$ (a nonzero v_e makes the gap even more anisotropic). The other is the regime of large δ , where the ratio $\tilde{\Delta}_e/\Delta_e$ is again large, but now because \tilde{u}_3 becomes the dominant interaction. In between, $\tilde{\Delta}_e/\Delta_e$ passes through minimum, at $\delta = \delta_{min}(\gamma)$. Near $\gamma = 1$, $\delta_{min}(\gamma) \approx \sqrt{\gamma-1}$, while for large γ , $\delta_{min}(\gamma) \approx (\sqrt{3}/2)\gamma$.

For $v_e \neq 0$, the phase diagram is the same as in Fig. 2, but the boundary of the nodeless phase shrinks to smaller γ , the crossover near the critical γ becomes more smooth, and the value of T_c in the region where the gap has nodes is larger. In particular, when $v_e \sim u_3$ and $\delta = \mathcal{O}(1)$, T_c in the regions where the gap has nodes and has no nodes are quite comparable.

Consider next B_{1g} pairing. Now $\Delta_e(q) = \pm \Delta_e$ with the sign change between the two electron FSs, while $\Delta_h(q) = \tilde{\Delta}_h(\cos q_x - \cos q_y) \approx \tilde{\Delta}_h \sqrt{2} \cos 2\phi$ with $\tilde{\Delta}_h = k_F^2 \tilde{\Delta}_h / 2\sqrt{2}$. The equations for Δ_e and $\tilde{\Delta}_h$ become

$$\tilde{\Delta}_h = -\tilde{u}_3 L \Delta_e, \quad \Delta_e = -\tilde{u}_3 L \tilde{\Delta}_h - (u_4 - v_e) L \Delta_e, \quad (5)$$

and T_c is given by $1 + (u_4 - v_e)L = \tilde{u}_3^2 L^2$, where, as before, $L = \ln \Lambda / T_c$. Again, the solution exists only if $v_e > u_4$ when $\tilde{u}_3 = 0$, but once $\tilde{u}_3 \neq 0$ it survives even for arbitrary strong u_4 repulsion. We compared $T_c^{s^\pm}$ and $T_c^{d_{x^2-y^2}}$ and found that for all values of parameters $T_c^{s^\pm}$ is larger although $d_{x^2-y^2}$ pairing is close second.

We also analyzed d_{xy} pairing, by expanding the interaction to next order (k_F^4). The d_{xy} gap $\Delta(q) \propto \sin q_x \sin q_y$ has nodes along both hole and electron FSs and is advantageous at large u_4 because u_4 completely disappears from the gap equation. We found that, for $v_e = 0$, $T_c^{B_{2g}}$ has the same dependence on k_F as T_c for A_{1g} case ($L \propto 1/k_F^4$) and becomes larger than $T_c^{A_{1g}}$ for large γ . However, for $v_e \neq 0$, s^\pm pairing wins for all u_4 because v_e sets a finite lower edge for T_c for an s^\pm gap and acts as a repulsive interaction for d_{xy} gap.

IV. ROLE OF IMPURITIES

The plus-minus s^\pm SC state at $\gamma < 1$ and $\delta \ll 1$ is suppressed by interpocket impurity scattering Γ_π (Refs. 5, 14,

and 16) but is not sensitive to a much stronger intrapocket impurity scattering Γ_0 . We now show that Γ_0 is pair breaking at $\gamma \gtrsim 1$ when superconductivity develops via \tilde{u}_3 . To evaluate the effect of Γ_0 on T_c , we derived the self-consistency equations within the Born approximation. For $v_e=0$, the equation for $T_c(\Gamma_0)$ becomes

$$(1 + u_4 L)^2 - u_3^2 L^2 = \tilde{u}_3^2 (1 + u_4 L) L \mathcal{L}(\Gamma_0), \quad (6)$$

where

$$\mathcal{L}(\Gamma_0) = \ln \frac{\Lambda}{T_c(\Gamma_0)} + \psi\left(\frac{1}{2}\right) - \psi\left(\frac{1}{2} + \frac{\Gamma_0}{2\pi T_c(\Gamma_0)}\right), \quad (7)$$

where $\psi(x)$ is the digamma function. Both the lhs and the rhs of Eq. (6) now scale as L^2 at $T_c \rightarrow 0$ because $\mathcal{L}(\Gamma_0)$ tends to a constant at $T_c=0$. As a result, the solution of Eq. (6) exists when \tilde{u}_3^2 exceeds the threshold set by Γ_0 .

V. APPLICATION TO THE Pnictides

Electron and hole pockets in the pnictides are rather small in size, and it is likely that $\delta \propto E_F/W$ is small. Our analysis shows that for small δ , two situations are possible. When the tendency to a nesting-driven SDW order is strong enough, the pair-hopping term u_3 gets a boost from SDW fluctuations and at energies of order E_F likely exceeds intrapocket repulsion u_4 , i.e., the system develops an attraction in an s^\pm channel which, taken alone, leads to s^\pm gap without nodes and with near-equal magnitudes along hole and electron FSs. In this situation, the leading instability of an undoped system is toward an SDW order, and a system becomes a supercon-

ductor only after spin order is destroyed by a finite doping.^{22,26} We believe that this scenario works for underdoped/optimally doped FeAs 1111 and 122 materials in which SDW fluctuations are well developed. When the tendency toward SDW order is weaker, u_4 remains the largest down to E_F , and a nodeless s^\pm gap does not develop. However, the angle-dependent part of the pair hopping u_3 between hole and electron FSs still gives rise to an s^\pm pairing, but now s^\pm gap has nodes along electron FSs. Furthermore, T_c for such state is enhanced by the pair hopping v_e between two electron FSs. This is our scenario for FeP-based LaOFeP which does not display a SDW order and for BaFe₂(As_{1-x}P_x)₂ in which SDW order disappears without doping. We conjecture that the same scenario (leading to the nodes in the gap) should also be valid for overdoped FeAs 1111 and 122 materials.

Note added: Recently, a functional RG study has been reported (Ref. 27), in which the angle-dependent part of the pair hopping has been included. The authors found an extended s -wave gap with nodes in exactly the same parameter range as in our analytical work.

ACKNOWLEDGMENTS

We acknowledge with thanks useful discussions with E. Abrahams, A. Carrington, I. Eremin, K. Haule, P. Hirshfeld, G. Kotliar, D-H. Lee, J-X. Li, T. Maier, Y. Matsuda, I. Mazin, R. Prozorov, D. Scalapino, J. Schmalian, D. Singh, and Z. Tesanovic. The work was supported by NSF Grant No. DMR-0604406 (A.Ch).

- ¹I. I. Mazin *et al.*, Phys. Rev. Lett. **101**, 057003 (2008).
- ²K. Kuroki *et al.*, Phys. Rev. Lett. **101**, 087004 (2008); V. Barzykin and L. P. Gorkov, JETP Lett. **88**, 131 (2008).
- ³Y. Bang *et al.*, Phys. Rev. B **79**, 054529 (2009).
- ⁴F. Wang *et al.*, Phys. Rev. Lett. **102**, 047005 (2009).
- ⁵A. V. Chubukov *et al.*, Phys. Rev. B **78**, 134512 (2008); A. Chubukov, Physica C **469**, 640 (2009).
- ⁶K. Kuroki and H. Aoki, Physica C **469**, 635 (2009).
- ⁷K. Seo *et al.*, Phys. Rev. Lett. **101**, 206404 (2008).
- ⁸S. Graser *et al.*, New J. Phys. **11**, 025016 (2009); T. A. Maier *et al.*, Phys. Rev. B **79**, 224510 (2009).
- ⁹M. Daghofer *et al.*, Phys. Rev. Lett. **101**, 237004 (2008); A. Moreo *et al.*, Phys. Rev. B **79**, 134502 (2009); Y. Yanagi *et al.*, J. Phys. Soc. Jpn. **77**, 123701 (2008); H. Ikeda, *ibid.* **77**, 123707 (2008); S.-L. Yu *et al.*, Phys. Rev. B **79**, 064517 (2009).
- ¹⁰K. Nakayama *et al.*, EPL **85**, 67002 (2009) and references therein.
- ¹¹X. G. Luo *et al.*, Phys. Rev. B **80**, 140503(R) (2009).
- ¹²K. Hashimoto *et al.*, Phys. Rev. Lett. **102**, 017002 (2009); L. Malone *et al.*, Phys. Rev. B **79**, 140501(R) (2009).
- ¹³R. T. Gordon *et al.*, Phys. Rev. Lett. **102**, 127004 (2009); C. Martin *et al.*, Phys. Rev. B **80**, 020501(R) (2009).

- ¹⁴A. B. Vorontsov *et al.*, Phys. Rev. B **79**, 140507(R) (2009).
- ¹⁵V. Mishra *et al.*, Phys. Rev. B **79**, 094512 (2009).
- ¹⁶D. Parker *et al.*, Phys. Rev. B **78**, 134524 (2008); O. V. Dolgov *et al.*, New J. Phys. **11**, 075012 (2009).
- ¹⁷J. D. Fletcher *et al.*, Phys. Rev. Lett. **102**, 147001 (2009); C. W. Hicks *et al.*, *ibid.* **103**, 127003 (2009).
- ¹⁸M. Yamashita *et al.*, arXiv:0906.0622 (unpublished).
- ¹⁹K. Hashimoto *et al.*, arXiv:0907.4399 (unpublished).
- ²⁰L. Boeri *et al.*, Phys. Rev. Lett. **101**, 026403 (2008).
- ²¹C. Platt *et al.*, New J. Phys. **11**, 055058 (2009).
- ²²V. Cvetkovic and Z. Tesanovic, Phys. Rev. B **80**, 024512 (2009).
- ²³The RG analysis for two hole and two electron FS has been performed by K. Haule (unpublished).
- ²⁴See, e.g., D. J. Singh, Phys. Rev. B **78**, 094511 (2008).
- ²⁵Alternatively, one can write A_{1g} component as $u_3^{A_{1g}}(\mathbf{q}, \mathbf{q}') \propto Y_{A_{1g}}(\mathbf{q})Y_{A_{1g}}(\mathbf{q}')$ with $Y_{A_{1g}}(\mathbf{q}) = 1 + b(\cos q_x + \cos q_y)$ (Ref. 8). This leads to the same set of gap equations as Eq. (2) but u_3 has to be multiplied by $(1+2b)$.
- ²⁶A. B. Vorontsov *et al.*, Phys. Rev. B **79**, 060508 (2009); J. Zhang *et al.*, *ibid.* **79**, 220502(R) (2009).
- ²⁷R. Thomale *et al.*, arXiv:0906.4475 (unpublished).